Composites Part B 146 (2018) 76–87

Contents lists available at ScienceDirect

Composites Part B

journal homepage: www.elsevier.com/locate/compositesb

Quantifying effects of graphene nanoplatelets on slowing down combustion of epoxy composites

Qiangjun Zhang[a], Yong C. Wang[a,*], Colin G. Bailey[b], Richard K.K. Yuen[c], Joshua Parkin[a], Wei Yang[c], Cristina Valles[a]

[a] University of Manchester, Oxford Rd, Manchester, M13 9PL, United Kingdom
[b] Queen Mary University of London, Mile End Rd, London, E1 4NS, United Kingdom
[c] City University of Hong Kong, 83 Tat Chee Ave, Kowloon Tong, Hong Kong

ARTICLE INFO

Keywords:
Graphene nanoplatelets
Combustion behaviour
Barrier effect
Pyrolysis simulation
Epoxy composites

ABSTRACT

This paper investigates the effects of graphene nanoplatelets (GNP) on combustion behaviour of epoxy resin (ER). In particular it presents, for the first time, a numerical modelling methodology that quantifies the effects of GNP in reducing the peak rate of heat release of epoxy resin with different amounts and types of GNP.

Five different GNP/ER composites were prepared via the solution mixing method. Geometric characteristics and dispersion state of GNP in epoxy resin were characterized by three-dimensional (3D) X-ray CT scan. Thermogravimetric analysis (TGA) tests were carried out on pure epoxy and GNP/ER composites in N_2. Bench-scale cone calorimeter tests were used to obtain combustion properties of the prepared nanocomposites. These test results provide input data for validating the modelling methodology.

The cone calorimeter tests found significantly lower peak heat release rate (PHRR) for GNP/ER composites than pure epoxy. For example, at 3 wt% GNP loading, the PHRR was reduced by 47%. This drastic reduction in PHRR due to GNP is attributed to two principal contributions of GNP: reduced permeability to slow down movement of volatiles to the surface to cause combustion, and reduced radiant conductivity of GNP/ER at high temperatures owing to GNP being able to promote the formation of a continuous and compact char layer, which decreases temperatures and hence slows down chemical reactions. This paper provides a new method, through numerical pyrolysis modelling, to quantify these two contributions and their effects in reducing PHRR of GNP/ER. A comparison between numerical simulation results and test results confirms assumptions of this quantitative method. This simulation model has the potential to improve material design process of graphene based composites and predict the fire behaviour of such composites in realistic fire conditions.

1. Introduction

With the growing demand for lighter, stronger and safer aircrafts, there has been considerable academic and industrial interest in graphene-based polymer composites. Since the discovery of graphene, a great number of researchers have been working on developing composite materials with graphene, hoping to transfer the superb properties of graphene from micro-scale nanosheets to macro-scale bulk composites. So far numerous studies have reported huge potential of graphene as reinforcement filler for polymers to achieve multiple performance improvements, including increased thermal and electrical conductivity and mechanical properties [1–4].

Fire hazard in aircrafts is a critical safety concern due to high flammability of polymer resins. An accidental electrical failure could start a fire, leading to potentially disastrous consequence for aircrafts. This concern has led many researchers to investigate combustion behaviour of epoxy composites with graphene and its derivatives. For example, Liu et al. [5] reported a 56.9% reduction in the peak heat release rate (PHRR) of epoxy composites with a loading of 5% by weight (1 wt%) of graphene nanosheets (GNS) in cone calorimeter testing. Jiang et al. [6], Wang et al. [7] and Wang et al. [8] arrived at similar findings for GNS/ER composites. Graphene oxide and reduced graphene oxide has also been shown to reduce PHRR of epoxy with a low loading of 1 wt% [9,10].

This suppression effect on PHRR by graphene was qualitatively explained by the so-called barrier effect in literature. Some researchers speculate that graphene flakes act as blocking walls to hinder the escape of gas volatiles during pyrolysis thereby slowing down combustion and hence lowering PHRR [8]. This explanation is qualitatively justifiable as graphene is reported to be impermeable even to helium and has been

* Corresponding author.
E-mail address: yong.wang@manchester.ac.uk (Y.C. Wang).

https://doi.org/10.1016/j.compositesb.2018.03.049
Received 12 January 2018; Received in revised form 16 February 2018; Accepted 30 March 2018
Available online 31 March 2018
1359-8368/

Nomenclature

E	Activate Energy (kJ/mol)
A	Pre-exponential factor (s^{-1})
n	Reaction order
PHRR	Peak heat release rate (kW/m^2)
EHC	Effective heat of combustion (MJ/kg)
PMLR	Peak mass loss rate (g/m^2 s)
K	Thermal conductivity (W/m K)
C	Specific heat capacity (J/kg K)
D	Characteristic dimension of pores (m)
ΔH	Heat of volatilization (J/kg)
k_a	Absorption Coefficient (m^{-1})
ε	Emissivity
α	Aspect ratio
ϕ	Volume Fraction of GNP in epoxy resin
τ	Tortuosity factor
σ	Reduced pore diameter factor
q	Mass flux per unit area (m/s)
ΔP	Pressure gradient (Pa/m)
k	Intrinsic permeability of the medium (m^2)
μ	Gas viscosity (Pa·s)
γ	Radiant conductivity
Ψ	Porosity
α_r	Conversion rate of thermal decomposition

reported to possess efficient gas barrier properties in different polymers [11]. Other researchers claim that the improved char structure after adding GNP will also contribute to better combustion performance of composites, particularly a lower PHRR [12].

Whilst it is intuitively correct to attribute reduced PHRR to barrier effects and improved char structure due to GNP, there has been no research to quantitatively demonstrate and explain the observed results. Without a quantitative model it would not be possible to design graphene based composites, nor be able to predict the behaviour of such composites in fire conditions. Providing a quantitative model that is able to calculate the reduced PHRR of graphene based composites is the main focus of this research.

Because different researchers have used different materials, it is difficult to use their data in a quantitative way for development of a prediction model due to a lack of some details. Therefore, in this study, the authors have carried out independent, and additional, tests for epoxy composites filled with different loadings and types of GNP, including X-ray CT scan, TGA, cone calorimeter and SEM of char.

In conventional combustion modelling related to fire safety, the pyrolysis gases are assumed to move instantly to the surface from inside the solid in order to reduce computation time. This assumption is acceptable for materials with high permeability. However, if material permeability is low, the time it takes for gas volatiles to move to the surface will have an important effect on peak combustion and it is important that this effect is considered in combustion modelling, as it is in the present paper.

This paper uses Gpyro [13] to simulate cone calorimeter tests. Gas movement inside the solid phase is simulated by Darcy's law and is controlled by gas permeability of GNP/ER composite and its char after combustion. Therefore, such a quantitative model to predict combustion behaviour of graphene modified composites requires data on the internal structure of the composite, which provides input to calculating gas permeability of the composite. Different GNP types with different geometric information will be added into epoxy resin to make different GNP/ER composites for comparison. Furthermore, radiant conductivity of the char will need to be taken into consideration for different char structures of GNP/ER.

The results of numerical pyrolysis modelling presented in this paper demonstrate validity of this model in quantifying the effects of GNP in reducing PHRR of epoxy, due to reduced permeability (barrier effect) and lower radiant conductivity (improved char structure). The numerical modelling approach provides the foundation to developing a comprehensive understanding of the fire performance of graphene-based epoxy nanocomposites which will be a powerful tool for future design of graphene modified composites for fire safety.

2. Experimental methods

2.1. GNP/ER composite samples

Three types of GNP (M5, M15, M25) were provided by XG Sciences in the U.S.A. Table 1 lists the geometric information of GNP. The epoxy and hardener were Araldite LY5052 and Aradur 5052 respectively. GNP was first sonicated in acetone for 2.5 h at a ratio of 1 mg per 1 ml. Epoxy was then added and sonicated for a further 2.5 h. After removing acetone and leaving only epoxy and GNP mixture, hardener was added to the mixture at a ratio of 100:47 (epoxy: hardener in volume). The mixture was then cast in moulds with dimensions of 100 mm × 100 mm with a thickness of 4 mm. Samples were left to cure for 24 h at ambient temperature followed by a further heated curing at 100 °C for 4 h.

Five different composites were made, as listed in Table 2. Composites #1, #2 and #5 have the same GNP (M15) type and investigate the effects of different GNP loading by weight (0.1 wt%, 1 wt% and 3 wt%). Composites #2, #3 and #4 investigate the effects of using different types of GNP (M5, M15 and M25) while maintaining the same loading by weight (1 wt%). Three samples of each composite were tested. Sample #0 is the reference case with pure epoxy without any GNP.

2.2. Tests

In total, four different types of tests were carried out: 3D X-ray CT scan, Thermogravimetric analysis (TGA), scanning electron microscopy (SEM) and cone calorimeter. 3D X-ray CT scans provide information of internal structures of the GNP/ER composites which can be used to assess the dispersion state of GNP/ER composites. The TGA results provide input data on mass loss rates and the cone calorimeter test results are used for validation of the pyrolysis modelling. The SEM test images provide qualitative information of char structures to aid assumptions of gas permeability and radiant conductivity of char.

2.2.1. 3D X-ray CT scan test

The ZEISS Xradia 810 Ultra XCT was used to observe the dispersion state and morphology of GNP inside epoxy resin. The field of view was 65 microns and the resolution was 50 nm.

2.2.2. Thermogravimetric analysis (TGA) test

Thermogravimetric analysis (TGA) was performed on a Netzsch TG

Table 1
Geometrical Characteristics of selected GNP materials.

	Average Lateral Size (μm)	Average Thickness (nm)	Density (g/cm^3)	Bulk Density (g/cc)
M5	5	6–8	2.5	0.03–0.1
M15	15	6–8	2.5	0.03–0.1
M25	25	6–8	2.5	0.03–0.1

Table 2
Formulation of GNP/ER composite.

Sample	Weight Fraction	GNP Type
#0	/	/
#1	0.1 wt%	M15
#2	1.0 wt%	M5
#3	1.0 wt%	M15
#4	1.0 wt%	M25
#5	3.0 wt%	M15

209 F1. Each TGA sample weighed 5–8 mg. Samples were tested from 30 to 800 °C with heating rate of 20 °C/min. Two parallel runs were performed for each sample. The tests were conducted under nitrogen.

2.2.3. Scanning electron microscopy test

After cone calorimeter testing, AMRAY1000B SEM tests were performed to obtain morphologies of the char surfaces.

2.2.4. Cone calorimeter test

The cone calorimeter tests were carried out at the City University of Hong Kong, using a FTT Cone Calorimeter. The cone calorimeter was calibrated according to ISO 5660 [14]. The sample size was 10 × 10 × 0.4 cm. A heat flux of 50 kW was applied during testing. When epoxy is heated, it expands and the top surface may touch the igniter leading to failure of the weighing device in the standard setup. To avoid this problem the distance between sample surface and heating hood was set to be 30 cm, which is 5 cm lower than the standard test setup. At this position, the actual heat flux on the surface of the sample was found to be 48 kW/m^2.

3. Experimental results and discussions

3.1. X-ray CT scan images of GNP/ER composites

Fig. 1 shows typical XCT images of epoxy composite with 1 wt% M25 GNP. It can be clearly found that GNPs were randomly dispersed in the epoxy matrix without noticeable aggregation. This confirms that the optimized preparation method for these nanocomposites was appropriate and successfully avoided flake aggregation which often is the main reason for deteriorated performance for nanocomposites. From the front side view in Fig. 1(b), the lateral sizes of GNP are mostly around 25 μm, in accordance with the specified GNP type in Table 1. However, the images also show a great amount of tiny GNPs in the composite. While the maximum value of lateral size of GNP is in line with the information of the supplier, the geometric information (M25) provided by the supplier is not able to represent the detailed geometric characteristics of GNPs in the composites.

3.2. TGA results

Fig. 2 presents the thermal degradation data from TGA tests for GNP/ER composites under N_2 atmosphere. All GNP/ER composites experienced only a single step decomposition process between 365 and 475 °C, the same as pure epoxy.

The char residues formed at the end of TGA tests are slightly higher for increased loading of GNPs in epoxy composites, as GNP tends to stay stable at high temperatures, thus retaining its original mass in the char residue. The DTG curves (Fig. 2b) clearly show that all samples reached similar peak mass loss rates, with 3 wt% GNP/ER showing a slightly lower peak mass loss rate (PMLR). These results demonstrate and confirm that GNP is chemically stable at high temperatures. Therefore, it is acceptable to assume that GNP will not be involved in the pyrolysis reaction of epoxy, which means that GNP/ER composites will exhibit the same decomposition path as pure epoxy. Thus, it is the physical changes in GNP/ER, rather than chemical reaction changes, that determine combustion behaviour of GNP/ER.

3.3. Cone calorimeter test results

Each GNP/ER composite had three samples and all cone tests were repeated three times. Fig. 3 shows results recorded for the three repeat cone tests for 1 wt% M25 GNP/ER composites. The recorded results are close, indicating consistency of the tests. The same trend has been observed for other cases.

Fig. 4 compares recorded heat release rate (HRR) and mass loss rate (MLR) – time curves of pure ER and GNP/ER composites from cone tests. For GNP/ER composites, different loadings (0.1 wt%, 1 wt% and 3 wt%) of the same GNP type (M15) and different types of GNP (M5, M15, M25) of the same loading (1 wt%) can be compared. All GNP/ER samples have lower PHRR compared to pure epoxy sample. In particular, epoxy composites with 3 wt% GNP had a 47% reduction in PHRR. Table 3 gives detailed quantities of PHRR, PMLR and effective heat of combustion (EHC). All samples have similar effective heat of combustion, which means that the total heat generated from combustion of per gram GNP/ER composite has not changed. This is expected because the

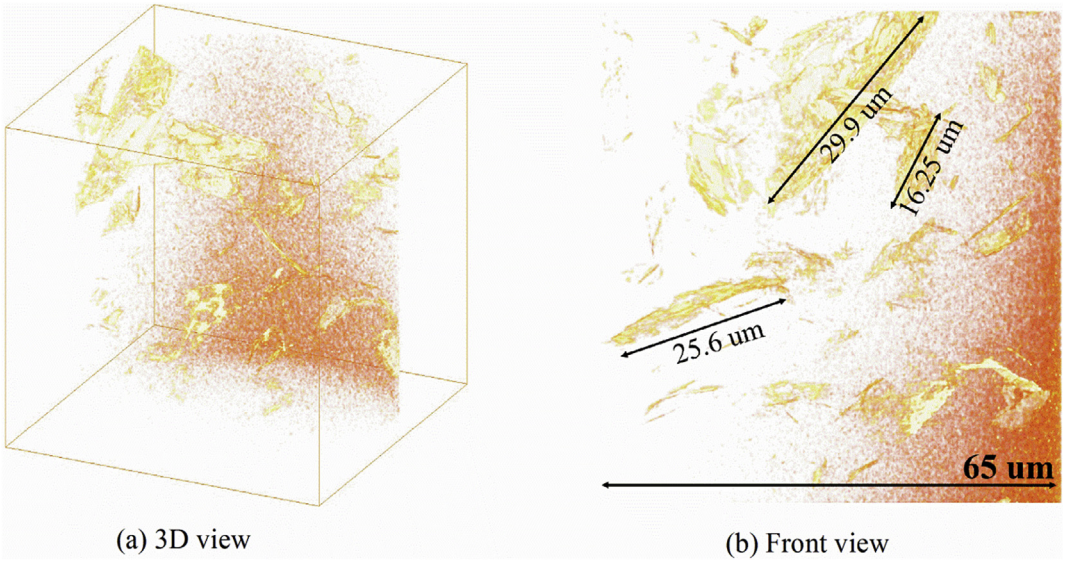

Fig. 1. XCT images of 1 wt% M25 GNP/ER composites.

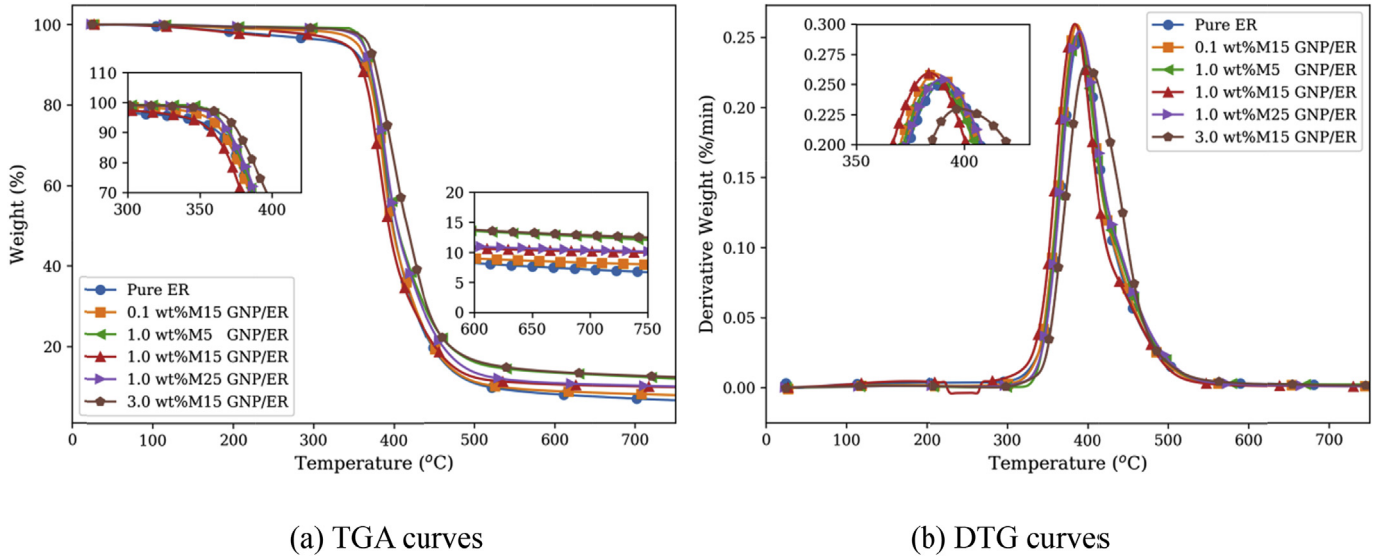

Fig. 2. TGA and DTG curves of GNP/ER composites under N_2.

GNP loading was very low in all cases. However, for the same total heat release, a lower PHRR means a lower fire hazard, because it is the PHRR that has a critical influence on fire and flame spreading.

It also shows that if GNP loading is the same, different types of GNP seem to have very similar effects on heat release, with results of PHRR and HRR – time curves being very similar for epoxy composites with M5, M15 and M25 GNP for 1 wt% loading.

The mass loss rates (MLR) recorded in the cone calorimeter tests indicate almost identical trends as HRR results. The % reduction in PMLR is similar to the % reduction in PHRR. This is expected because mass loss records the amount of gas volatiles released from the sample and it is the gas volatiles that are combusted to release heat. However, the drop of PMLR was not found from MLR in TGA tests for various GNP/ER samples. This clearly indicates that it is not appropriate to use TGA results when assessing combustion behaviour of GNP/ER.

Combustion of gas volatiles generates CO and CO_2. Therefore, CO_2 and CO can also reflect the effects of GNP in composites. Fig. 5 further confirms that a similar trend as heat release can be found for CO and CO_2 gas production rates of pure ER and GNP/ER composites from cone calorimeter tests. These results indicate that the GNPs in Epoxy do not interfere with the chemical reaction process, with the result that the chemical formula of the volatiles released are the same as for pure epoxy. Also the GNPs only exist in the solid phase, so they do not promote soot formation in the gas phase reaction.

The difference in MLR obtained from TGA and cone calorimeter tests can be attributed to the difference in barrier effects of GNP in epoxy at different scales and with different boundary conditions, as well as different heating conditions. Fig. 6 shows the combustion process of cone calorimeter test and Fig. 7 illustrates the tortuous route of gas movement inside the cone and TGA testing samples. Due to large planar size of the cone calorimeter test, which represents realistic conditions, gas volatiles do not move horizontally and can only move in the vertical direction. GNP makes gas volatile movement in this direction tortuous, and thus drastically slows down gas volatiles escaping from the sample. In contrast, a TGA sample is tiny and has comparable dimensions in all directions. Gas volatiles can escape from the sample from all directions, as illustrated in Fig. 7, and almost instantaneously because the travel distance is very short. Therefore, even though there is still a gas barrier effect in the TGA sample, this barrier effect is tiny compared to a cone calorimeter sample. Furthermore, the TGA sample is uniformly heated

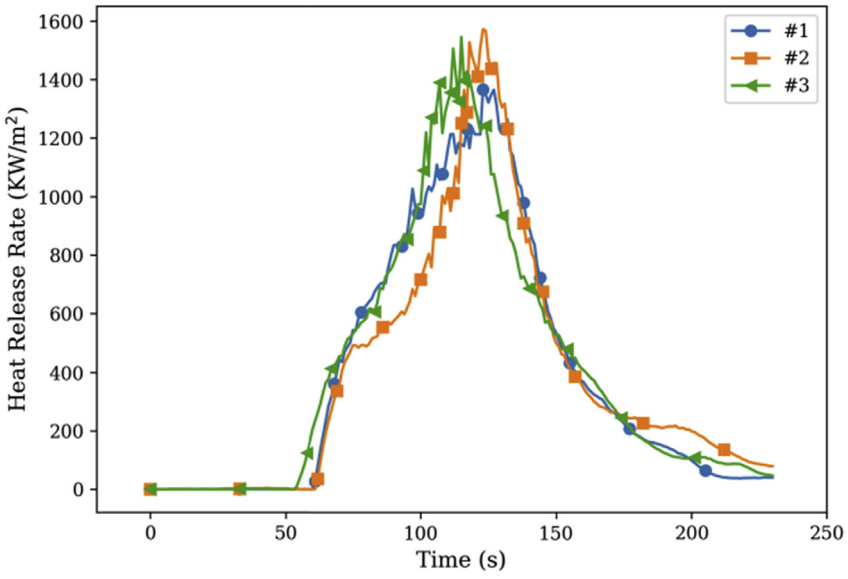

Fig. 3. Heat release rates from three repeat cone tests for 1 wt% M25 GNP/ER composite.

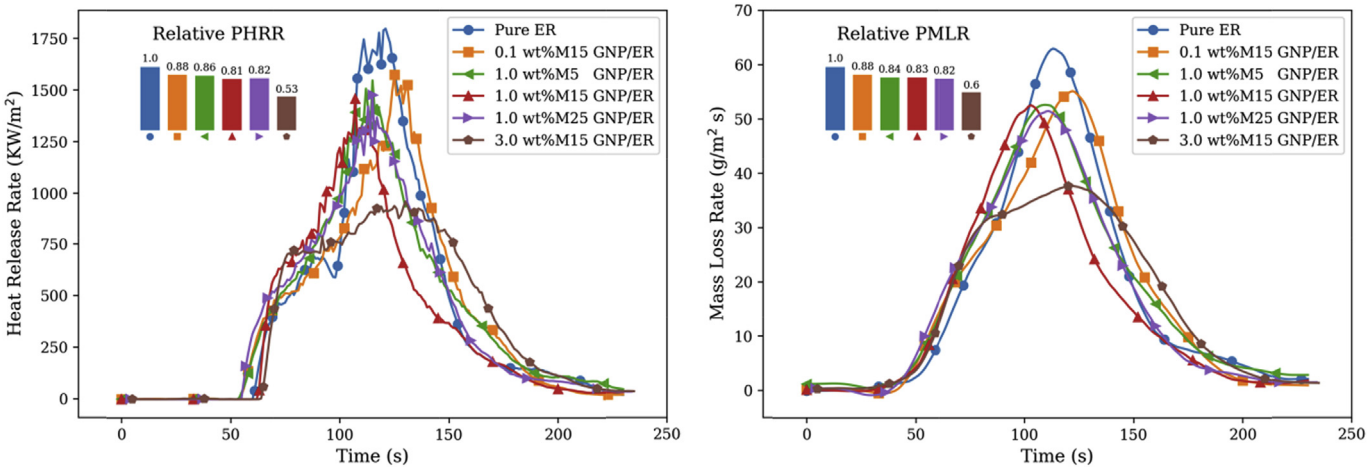

Fig. 4. Heat release rates and Mass loss Rate of pure ER and GNP/ER composites from cone tests.

Table 3
Combustion data of pure ER and GNP/ER composites from cone calorimeter tests.

Sample	PHRR kW/m²	PMLR g/m² s	EHC MJ/kg
Pure ER	1795.98	62.9	23.67
0.1 wt% M15 GNP/ER	1572.18	55.1	23.09
1.0 wt% M5 GNP/ER	1545.11	52.6	22.78
1.0 wt% M15 GNP/ER	1456.13	52.5	23.08
1.0 wt% M25 GNP/ER	1474.61	51.4	23.29
3.0 wt% M15 GNP/ER	958.48	37.6	22.82

which means the temperature gradient is negligible. Therefore, the heat transfer process cannot be reflected in this scale of a TGA test.

3.4. Char structure

Fig. 8 compares macro morphologies of char residues from different samples after cone calorimeter testing. They show improved char formation as GNP loading increases.

For pure epoxy and 0.1 wt% GNP/ER composites, very little char can be observed. For epoxy composites with 1 wt% GNP, a similar char layer was formed as for the 3 wt% GNP/ER composite. However, it was not strong enough to withstand pressure of the accumulated gases from pyrolysis underneath, and as a result, gas holes formed. For composites with 3 wt% GNP/ER, the char residue indicates a continuous and compact layer, acting like a protective layer for the layer below. The cracks on the surface were generated afterwards when taking the sample out from the cone testing sample holder.

Figs. 9 and 10 show detailed images of char structures from SEM tests. They show that for pure epoxy resin, only some tiny char particles could be seen on the foil sheet. For samples containing higher loading of GNP, it reveals that GNP-like platelets overlapped each other and formed a compact and continuous protective layer especially for the highest (3%wt) loading GNP samples, while uncovered holes existed in lower loading GNP samples. This overlapping and vertically-concentrated GNP dispersion can generate severe tortuous effect than normal random dispersion, and this can contribute to very low gas permeability for chars with high GNP loading.

The experimental results of this paper, in terms of mass loss rate from TGA tests and rate of heat release rate from cone calorimeter tests, concur with existing test results by others [5–8,15–17]: TGA test results showing similar changes in mass loss rate as GNP loading, while cone calorimeter test results giving drastically lower peak heat release rates and mass loss rates. The XCT and SEM images indicate that there are two contributions to graphene effects: GNP in epoxy forcing gas volatiles to move in tortuous paths inside GNP/ER composites and GNP helping to improve char structure which slows down heat transfer inside the GNP/ER composite.

4. Quantification of GNP contribution to slowing down combustion of epoxy

The above experimental results confirm the observations of others

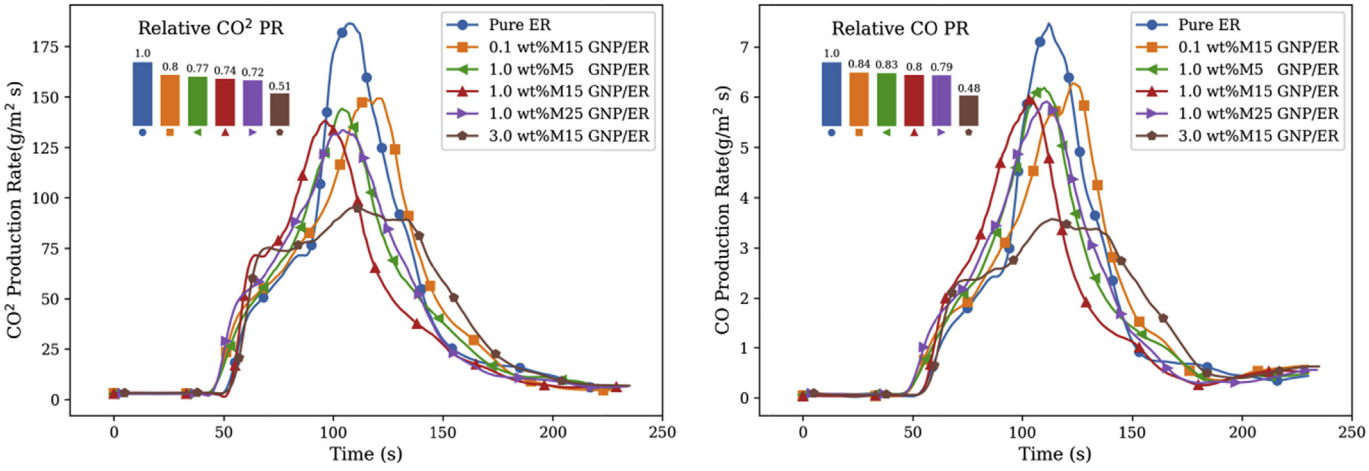

Fig. 5. CO and CO_2 production rates of pure ER and GNP/ER composites in cone tests.

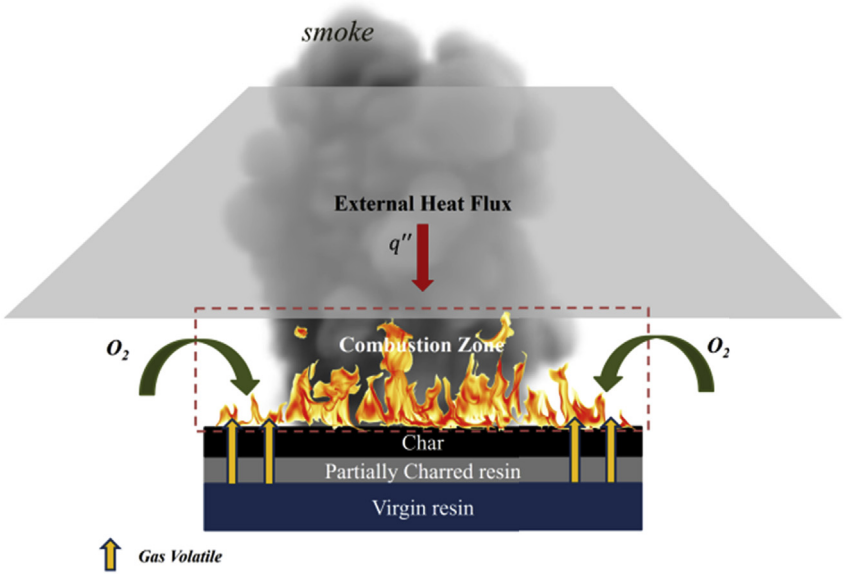

Fig. 6. Illustration of combustion process of epoxy sample in cone test.

that GNP can drastically decrease PHRR of GNP/ER and stipulate two contributory factors: tortuous effect that hinders gas volatile movement and improved char structure that slows down heat transfer. Due to experimental limitations, it is not technically possible to experimentally observe and quantify contributions of these two effects to slowing down combustion of GNP/ER. Therefore, numerical simulations are applied. The summary preliminary results presented in this section give confidence to the authors' proposed methodology of investigation.

4.1. Assumptions and parameter optimization

From the cone tests, different GNP/ER and pure ER samples have the same effective heat of combustion (EHC), which means a per gram sample of different composites will generate the same total amount of combustible gases for combustion. Since HRR is directly controlled by MLR (as discussed in the previous section), the previously presented TGA results of similar MLRs, and cone results of drastically lower MLRs in GNP/ER of high GNP loading, support the assumption that the fire suppression effects of GNP in epoxy only occur within the solid phase. Therefore, the quantification of GNP effects on slowing down combustion of GNP/ER will focus on predicting MLR during the generation and movement of gas volatiles of the pyrolysis process. In this paper, pyrolysis modelling was conducted by using the open source software Gpyro [13]. The TGA results were used to parameterize epoxy decomposition kinetics. As the MLR curves in Fig. 2(a) have shown, a single-step global reaction can be used to represent the epoxy pyrolysis process as follows.

$$\text{Epoxy} \rightarrow \text{Gas volatiles} + \text{Residue} \tag{1}$$

The reaction rate is assumed to be controlled by Arrhenius' equation:

$$\frac{d\alpha_r}{dt} = Ae^{-\frac{E}{RT}}(1-\alpha_r)^{n-1} \tag{2}$$

where α_r stands for conversion rate. The required kinetics (active energy, pre-exponential factor, reaction order) data can be extracted from the TGA test results under nitrogen through curve fitting, using the Gpyro 0D TGA model. The results in Table 4 were obtained.

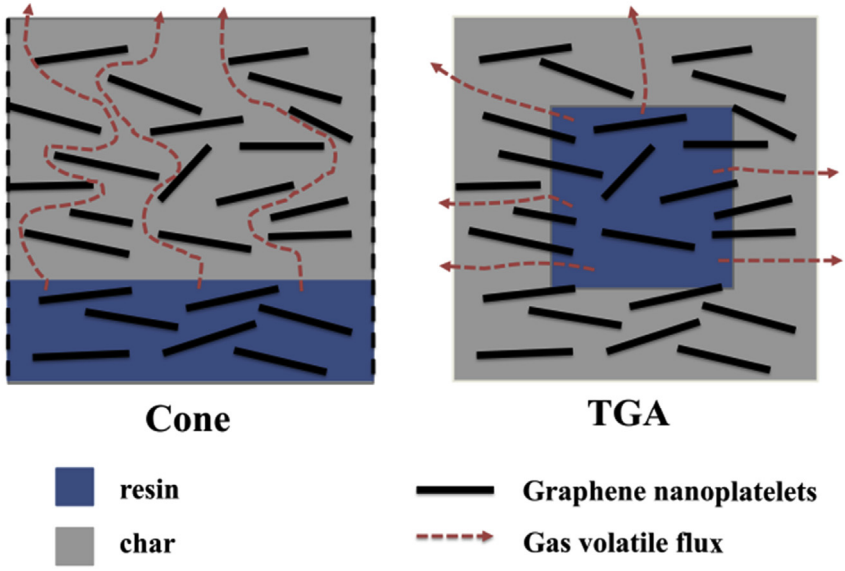

Fig. 7. Tortuous effect in cone test and free movement in TGA test.

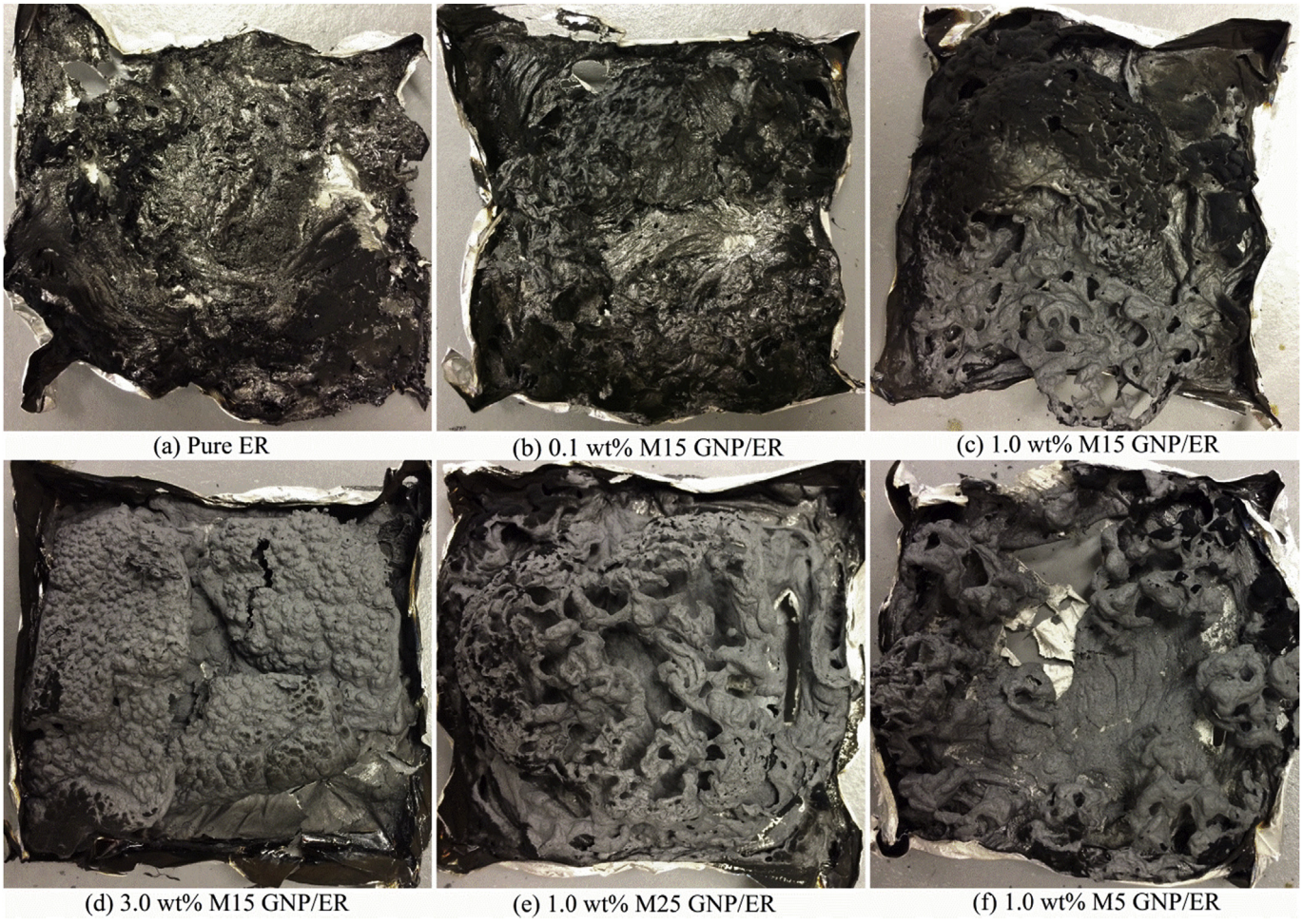

Fig. 8. Images of char structures of GNP/ER composites after cone calorimeter test (dimension = 10 cm × 10 cm).

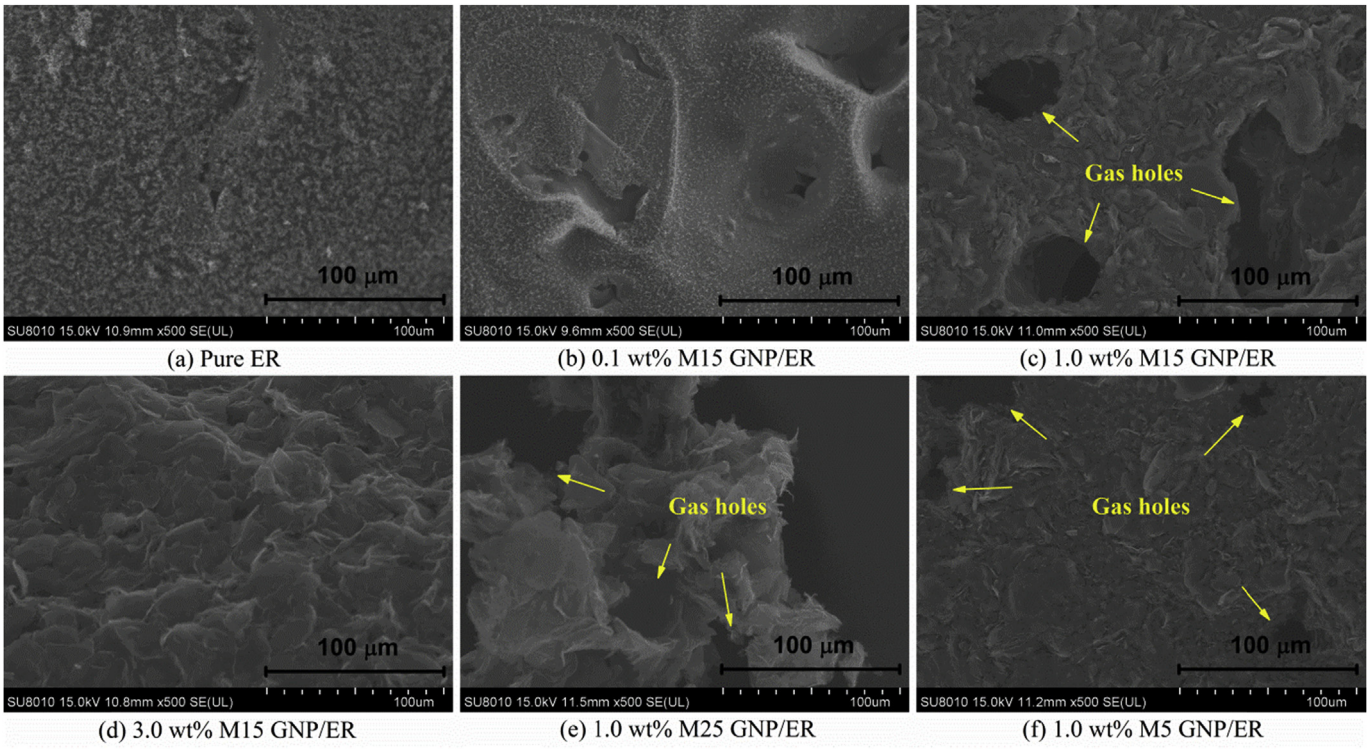

Fig. 9. SEM images of char from Pure ER and GNP/ER composites after cone calorimeter test (100 μm).

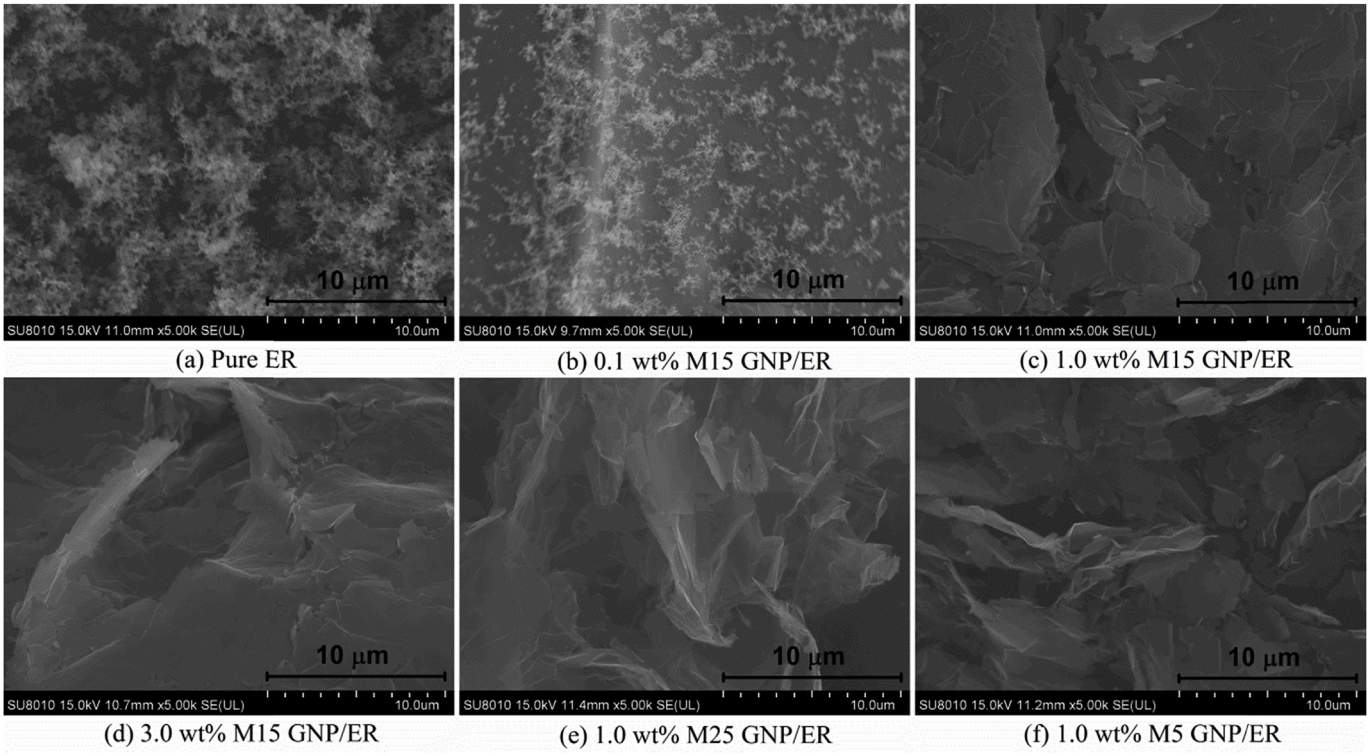

Fig. 10. SEM images of char from Pure ER and GNP/ER composites after cone calorimeter tests (10 μm).

Table 4
Kinetics for thermal decomposition reaction of epoxy resin.

Activate Energy (E) kJ/mol	Pre-exponential factor (A) s^{-1}	Reaction order (n)
1.81E15	240	2

According to TGA test results, GNP is assumed to be chemically stable during the pyrolysis process and does not influence thermal decomposition reaction of epoxy resin. Hence, the same kinetics will be applied to GNP/ER composites.

In order to perform numerical simulation of combustion of pure epoxy and GNP/ER composites using Gpyro, values of a number of thermal and physical parameters of epoxy are necessary. Epoxy has different varieties, and some of the required thermal and physical parameters are difficult or impossible to measure. In order to have reliable input data for modelling, a parameter optimization was performed. In this process, values of the required thermal and physical parameters were estimated, based on studies by others wherever available, or analytical relations with other quantities. Parameter optimization was then carried out through a genetic algorithm (GA) so that the simulated MLR histories for pure epoxy using the final input values of thermal and physical properties agree with cone tests.

The bulk density of epoxy resin is 1100 kg/m^3, which is calculated from the weight and volume of pure epoxy samples. The charring rate is about 5% according to cone testing results. The Emissivity (ε) and Absorption coefficient (k_a) are set to be 0.95 and 2700 (m^{-1}) respectively for both pure epoxy and char [13].

The oxygen permeability coefficient of pure epoxy is reported to be 2 cm^3 μm/(m^2 24 h mmHg) [18]. The relevant gas permeability (k) of pure epoxy is then calculated (Equation (7)) to be 1E-24 m^2 for oxygen with a viscosity (μ) of 2.04×10^{-5} Pa s [19]. This low gas permeability of pure epoxy means gas advection is unlikely to occur inside epoxy resin, as the porosity of pure epoxy is very low. Instead, slow gas diffusion would be the main mass transfer mode for gases inside the epoxy resin.

The gas permeability of the char formed after combustion of epoxy is difficult to measure. The char structure is similar to graphite material, so a gas permeability of 1E-15 m^2 of porous graphite matrix can be taken as a referenced value [20]. This reported gas permeability is measured with Nitrogen. Because pyrolysis gases from epoxy resin have much lower gas viscosity, an optimized gas permeability value for char is set to be 1E-16.

Table 5 lists other thermal and physical parameters, and compared values collected from literature and optimized values. Because Gpyro does not simulate combustion, a time dependent boundary condition was set to simulate heat feedback from the high temperature flame. At the start, the heat flux on the sample surface was 48 kW/m^2. After ignition, an extra 15 kW/m^2 was added to the surface to account for surface combustion [21].

From the data in Table 5, it can be found that the thermal conductivity and specific heat capacity values of epoxy and char after GA optimization are still close to the data from literature. For heat of volatilization (pyrolysis reaction), the optimized value is much lower than the reference value [25]. This may be due to different testing conditions. The reference value of ΔH was based on tests under Nitrogen. However, the cone tests were conducted in air with an abundant supply of oxygen, which will significantly decrease the amount of heat needed to pyrolysize epoxy [26]. The reference value of radiant conductivity is calculated by an empirical model (Equation (4)) combined with

Table 5
Thermal and physical parameters of epoxy resin from literature and GA optimization.

Parameter	After GA	Referenced Value
K_{epoxy} (W/m K)	0.335	0.346 [22]
C_{epoxy} (J/kg K)	1748	1700 [22]
K_{char} (W/m K)	0.219	0.2 [23]
C_{char} (J/kg K)	1294	1000 [24]
γ_{char}	0.0394	Equation (4)
Δ H (J/Kg)	170000	2400000 [25]

observed geometry of char for a pore diameter of char of about 2.5 mm.

Fig. 11 shows the Gpyro simulation results using the input data in Table 5 after GA optimization with experimental results for mass loss rate history of pure epoxy. The agreement is excellent, which provides a good starting point for later simulations for GNP/ER composites.

4.2. Numerical quantification of GNP effects on slowing down combustion of epoxy

4.2.1. Effect on thermal conductivity

The experimental results demonstrate that the existence of GNP was able to improve the char structure of GNP/ER compared to that of pure epoxy. This effect can be described by the contribution to radiant conduction in the porous char. The effective thermal conductivity (including both conductivity of air and thermal radiation in gas pores) is [27]:

$$K(T) = K_s(T) + K_r(T) = K_s\left(\frac{T}{T_r}\right)^{n_k} + \gamma\,\sigma\,T^3 \tag{3}$$

where $K_s(T)$ and $K_r(T)$ are solid thermal conductivity and radiant conductivity respectively. The latter one is attributed to radiation heat transfer across pores and is the dominant mode of heat transfer at high temperatures for highly porous materials such as the char of GNP/ER.

The coefficient for radiant conductivity γ is determined as [28]:

$$\gamma = \frac{13.5}{\varepsilon\,\Psi}D \tag{4}$$

where ε and Ψ are emissivity and porosity respectively; D is the characteristic dimension of pores (diameter for spherical pores and the maximum length for slots in the direction of heat transfer). A value of $\gamma_{char} = 0.0394$ in Table 5 corresponds to a pore characteristic dimension of 2.5 mm for the epoxy char, which is reasonable based on the image in Fig. 8. Images of char structures of GNP/ER show reduced pore diameters (D) of chars with increasing GNP loading. Using σ to define the ratio of pore characteristic dimension of GNP/ER char to ER char, then:

$$D_{char\ of\ GNP/ER} = \sigma(\phi,\ \alpha)\,D_{char} \quad (0 < \sigma < 1) \tag{5}$$

$$\gamma_{char\ of\ GNP/ER} = \sigma(\phi,\ \alpha)\,\gamma_{char} \quad (0 < \sigma < 1) \tag{6}$$

$\sigma(\phi,\ \alpha)$ is a function of the GNP volume fraction and aspect ratio.

For partially decomposed composite, the effective thermal conductivity is calculated based on volume fractions of unburnt and charred composites.

4.2.2. Gas permeability - barrier effect of GNP

The gas permeability of char and resin determine the speeds of gas volatiles generated during the pyrolysis moving within the porous media substance. In Gpyro simulation, movement of gas volatiles inside solid phases (char and resin) is controlled by Darcy's Law:

$$q = -\frac{k}{\mu}\nabla P \tag{7}$$

where q (m/s) is mass flux per unit area, ∇P (Pa/m) is the pressure gradient driving gas movement, k (m^2) is intrinsic permeability of the medium, and μ (Pa·s) is gas viscosity.

It has been widely acknowledged, and as demonstrated in Fig. 7, that the presence of GNP generates tortuous effects for gas movement in composites. For unburnt composites, introducing a tortuosity factor $\tau(\phi, \alpha)$ to represent the increased tortuous effect caused by GNP on ER compared to that of pure ER, as:

$$k_{GNP/ER} = \tau(\phi,\ \alpha)\,k_{ER} \quad (0 < \tau < 1) \tag{8}$$

For GNP/ER char, since GNP reduces pore sizes, gas permeability of char of GNP/ER is further reduced because when the pore size decreases, the resistance to gas flow increases. Since movement of gas volatiles is mainly through pores inside material, it is reasonable to assume that gas permeability is proportional to the pore size, as suggested by other researchers [29]. Therefore, the gas permeability of GNP/ER char can be related to that of ER as follows:

$$k_{char\ of\ GNP/ER} = \tau(\phi,\ \alpha)\,\sigma(\phi,\ \alpha)\,k_{char\ of\ ER} \quad (0 < \tau,\ \sigma < 1) \tag{9}$$

where $\tau(\phi,\ \alpha)$ accounts for tortuosity factor and $\sigma(\phi,\ \alpha)$ represents pore diameter reduction factor.

For partially decomposed composite, its gas permeability can be calculated based on volume fractions of unburnt and charred composites.

4.2.3. Results of sensitivity study

As has been mentioned in Section 4.1, GNP affects combustion of epoxy, and other composites, by the barrier effect of reduced gas permeability and improved char structure whereby the effective thermal conductivity is reduced. Although both effects have been mentioned and speculated by other researchers based on experimental results, it is interesting to examine their relative contributions.

Fig. 12 presents relative PMLR (ratio of PMLR of GNP/ER to PMLR of ER) for different values of τ (reduced permeability due to barrier effect) and σ (reduced effective thermal conductivity). It is clear that both effects are important in reducing PMLR of GNP/ER.

4.2.4. Modelling of cone calorimeter tests for GNP/ER composites

The tortuous effect of 2D platelets filler inside polymer matrix has been investigated by a number of researchers, and several empirical analytical models have been developed to predict gas permeability of composite materials [30–37]. Among them, the model developed by Bharadwaj [35] for randomly dispersed platelets with a high aspect ratio was used in this research to calculate a reference value for tortuous factor of GNP/ER composites.

The Bharadwaj equation is given by:

$$\tau = \frac{1-\phi}{1+\frac{\alpha\,\phi}{6}\left(s+\frac{1}{2}\right)} \tag{10}$$

where α is the GNP aspect ratio, ϕ is GNP volume fraction, s is 0 for randomly dispersed GNP. As mentioned earlier (Section 3.1), the supplier's data can be used for the calculating of α. Therefore, for M25, M15 and M5 GNP with an average thickness of 7 μm (Table 1), α = 3570, 1875 and 714 respectively. The volume fraction of GNP in ER is suggested to be half of weight fraction of GNP in ER, as the density of GNP is about two times of the density of ER.

At this stage it is not possible to accurately estimate the equivalent pore diameter of char of ER without and with GNP. However, it is possible to state that the pore size of GNP/ER char with a high GNP loading of 3 wt% is about one order of magnitude smaller than that pure ER. For 3 wt% GNP/ER (Fig. 8d), the char consists of a great number of tiny unbroken bubbles. However, for lower loading GNP/ER

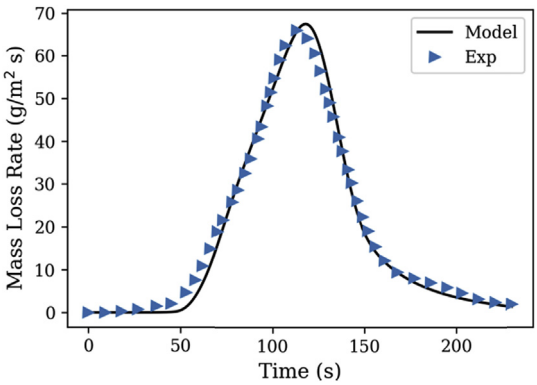

Fig. 11. Comparison for mass loss rate (MLR) between Gpyro prediction using GA optimization input data and experiment for pure epoxy.

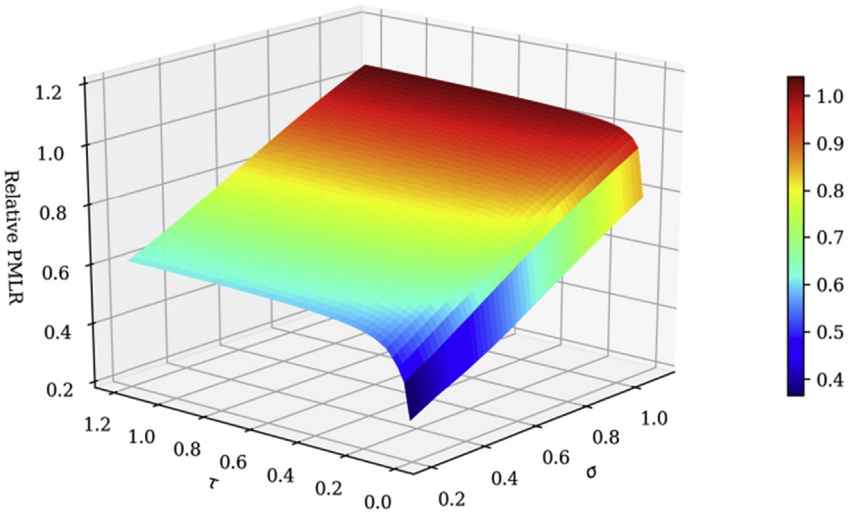

Fig. 12. PMLR Sensitivity to τ and σ

samples, much bigger gas holes can be found. A maximum value of 5 is assumed for the ratio of pore size of pure ER char to pore size of 3 wt% GNP/ER char, so a pore size of 0.5 mm (2.5mm/5) was used to calculate the radiant conductivity of GNP/ER char for 3 wt% loading. For other GNP loadings, inverse modelling was used to determine σ. For 1 wt% GNP/ER samples, the same value of σ was used for different aspect ratios, suggesting that it is the loading of GNP that will be the primary factor affecting the char structure of GNP/ER.

Table 6 lists the estimated σ and τ values. The relevant gas permeability and radiant conductivity can then be calculated with estimated value of σ and τ.

Based on the input data in Tables 5 and 6, mass loss simulations were carried out for the cone test samples using Gpyro. Fig. 13 compares the simulation and test results. Fig. 13 shows very good agreement between simulation experimental results for both mass loss rate (MLR) histories and peak mass loss rate (PMLR) for all cases.

4.3. Limitations

It is important to mention that modelling combustion behaviour of GNP/ER is extremely complex. Accurate modelling requires accurate input data and such data do not exist in literature and cannot be quantified experimentally. This paper has explained how these input data have been estimated to the best of the authors' understanding. Therefore, there are inevitable uncertainties in these input data. Nevertheless, this proposed quantitative method has been demonstrated to be capable of predicting pyrolysis behaviour for different GNP/ER samples and providing consistent quantitative explanations for GNP to slow down combustion of epoxy composites.

5. Conclusions

This paper has presented the results of a comprehensive combined experimental and numerical modelling study to quantify the heat and gas barrier effects of GNP on combustion behaviour of epoxy composites. A total of 5 GNP/ER composites were investigated, including M15 GNP loading of 0.1 wt%, 1 wt% and 3 wt% and M25 and M5 GNP loading of 1 wt%. The tests include X-ray CT scan, TGA, cone calorimeter and SEM. The open source software Gpyro was used to simulate pyrolysis of the composites. Based on experimental results of this research, the following conclusions can be drawn:

(1) The XCT scan images show that GNP was well dispersed in epoxy resin, no aggregation occurred.

(2) The TGA and cone calorimeter test results reveal very similar trends compared to existing test results by others: with TGA test results showing a similar change in mass loss rate with different GNP loading, while cone calorimeter test results give drastically lower PHRR, particularly for high GNP loading (3 wt%). Clearly it is not correct using TGA results as direct input when simulating combustion behaviour of GNP/ER composites: fast mass transfer from the edges and uniform temperature of TGA samples do not reflect conditions under cone testing.

(3) The XCT and SEM images indicate that there are two contributions to GNP effects: GNP in epoxy forcing gas volatiles to move in tortuous paths inside GNP/ER composites and GNP helping to improve the char structure with smaller pore diameter, thus decreasing radiant conductivity leading to lower temperature rise and slower chemical reaction. At 3 wt% GNP loading, the char structure appeared compact and continuous with a pore size about one order of magnitude smaller than that of pure epoxy.

(4) TGA test results indicate similar pyrolysis process for GNP/ER composites and pure epoxy. Therefore, GNP can be considered to not take part in chemical degradation reactions of epoxy. Hence, the same kinetics properties for pyrolysis reactions as pure epoxy can be used for GNP/ER composites.

(5) A method has been proposed to estimate a number of thermal and physical parameters required to simulate combustion behaviour of pure epoxy and GNP/ER composites, based on available values in literature or analytical relations with other parameters, in conjunction with a parameter optimization process for pure epoxy. For GNP/ER, a particularly important contribution of this research is the introduction of two reduction factors (Equations (6), (8) and (9)): the tortuosity factor for the physical barrier effect of GNPs in epoxy and the pore diameter factor for the heat barrier effect of GNPs in producing improved char.

(6) Using the thermal and physical parameters estimated as described above, the Gpyro simulation results are in very good agreement

Table 6
Estimated τ and σ values of GNP/ER composites.

	Pure ER	0.1 wt% M15 GNP/ER	1.0 wt% M15 GNP/ER	3.0 wt% M15 GNP/ER	1.0 wt% M25 GNP/ER	1.0 wt% M5 GNP/ER
α	0	1875	1875	1875	3570	714
ϕ	0	0.05%	0.5%	1.5%	0.5%	0.5%
τ	1	0.869	0.398	0.179	0.26	0.65
σ	1	0.7	0.6	0.2	0.6	0.6

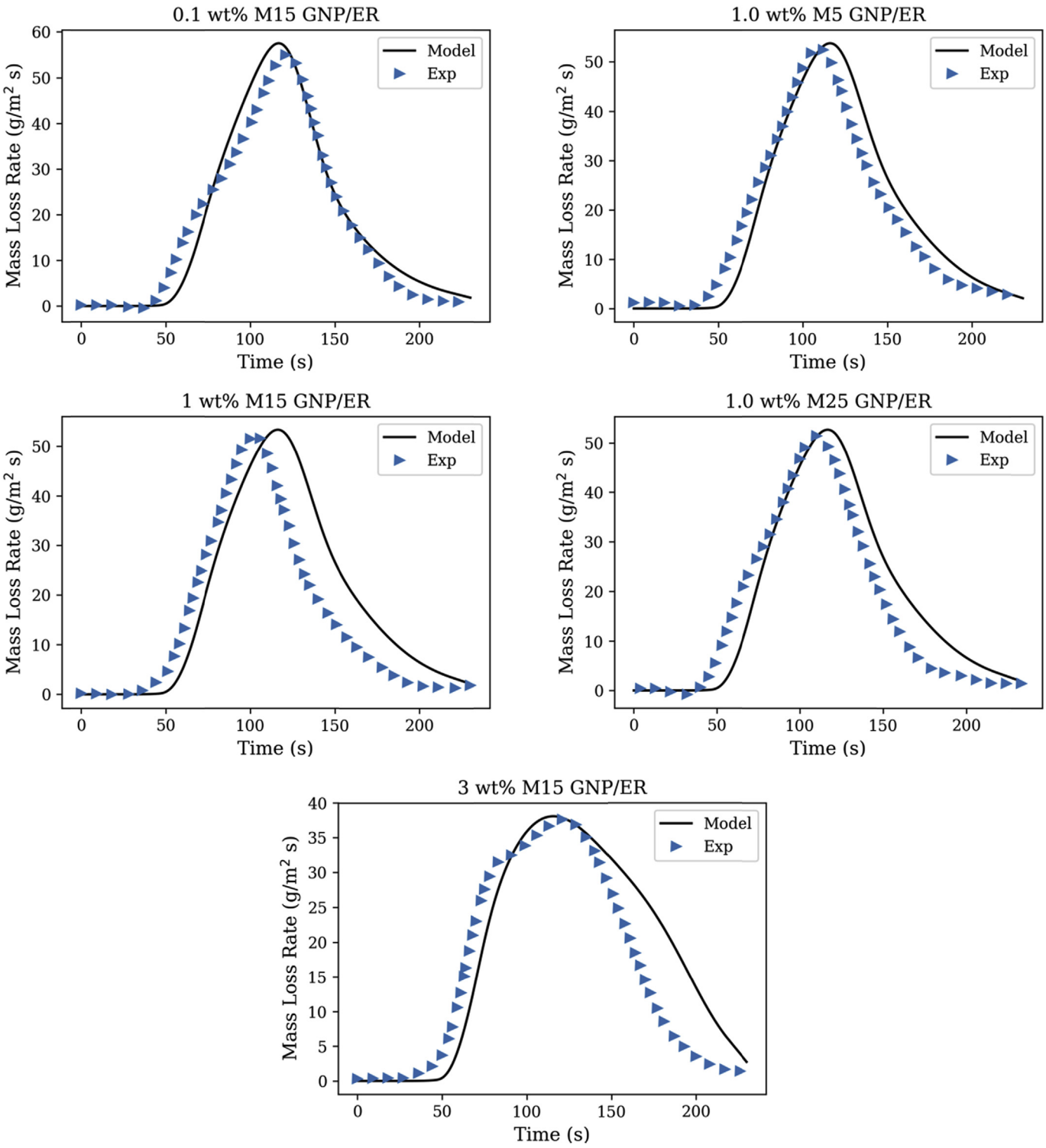

Fig. 13. Comparison of predicted MLR and cone test results.

with cone test results for mass loss rate (MLR) – time relationships, including PMLR. As HRR is directly controlled by mass loss rate (MLR), the same good agreement exists for HRR.

(7) Whilst there are considerable uncertainties in calculating gas permeability and radiant conductivity of both unburnt and partially decomposed epoxy and GNP/ER composites, the results of the preliminary numerical modelling of this research indicate feasibility of the proposed approach of obtaining composite thermal and physical parameters and equally importantly, of being able to quantitatively explain the physical and heat barrier effects of graphene in reducing PHRR of GNP/ER composites.

Acknowledgements

This work was supported by a University of Manchester President's Doctoral Scholar Award to the first author. The authors would like to thank Dr. James Baker, Prof Ian Kinloch, Prof Constantinos Soutis and Dr. Zheling Li for helpful discussions. We are also grateful to Dr Julia

Behnsen for assistance with XCT imaging.

Appendix A. Supplementary data

Supplementary data related to this article can be found at http://dx.doi.org/10.1016/j.compositesb.2018.03.049.

References

[1] Balandin AA, Ghosh S, Bao WZ, Calizo I, Teweldebrhan D, Miao F, Lau CN. Superior thermal conductivity of single-layer graphene. Nano Lett 2008;8:902–7.
[2] Rafiee MA, Rafiee J, Wang Z, Song HH, Yu ZZ, Koratkar N. Enhanced mechanical properties of nanocomposites at low graphene content. ACS Nano 2009;3:3884–90.
[3] Papageorgiou DG, Kinloch IA, Young RJ. Graphene/elastomer nanocomposites. Carbon 2015;95:460–84.
[4] Zakaria MR, Kudus MHA, Akil HM, Thirmizir MZM. Comparative study of graphene nanoparticle and multiwall carbon nanotube filled epoxy nanocomposites based on mechanical, thermal and dielectric properties. Compos B Eng 2017;119:57–66.
[5] Liu S, Fang ZP, Yan HQ, Wang H. Superior flame retardancy of epoxy resin by the combined addition of graphene nanosheets and DOPO. RSC Adv 2016;6:5288–95.
[6] Jiang SD, Bai ZM, Tang G, Song L, Stec AA, Hull TR, Zhan J, Hu Y. Fabrication of Ce-doped MnO2 decorated graphene sheets for fire safety applications of epoxy composites: flame retardancy, smoke suppression and mechanism. J Mater Chem A 2014;2:17341–51.
[7] Wang D, Zhou KQ, Yang W, Xing WY, Hu Y, Gong XL. Surface modification of graphene with layered molybdenum disulfide and their synergistic reinforcement on reducing fire hazards of epoxy resins. Ind Eng Chem Res 2013;52:17882–90.
[8] Wang X, Zhou S, Xing WY, Yu B, Feng XM, Song L, Hu Y. Self-assembly of Ni-Fe layered double hydroxide/graphene hybrids for reducing fire hazard in epoxy composites. J Mater Chem A 2013;1:4383–90.
[9] Wang R, Zhuo DX, Weng ZX, Wu LX, Cheng XY, Zhou Y, Wang JL, Xuan BW. A novel nanosilica/graphene oxide hybrid and its flame retarding epoxy resin with simultaneously improved mechanical, thermal conductivity, and dielectric properties. J Mater Chem A 2015;3:9826–36.
[10] Liu XW, Wu WH, Qi YX, Qu HQ, Xu JZ. Synthesis of a hybrid zinc hydroxystannate/reduction graphene oxide as a flame retardant and smoke suppressant of epoxy resin. J Therm Anal Calorim 2016;126:553–9.
[11] Berry V. Impermeability of graphene and its applications. Carbon 2013;62:1–10.
[12] Ran SY, Chen C, Guo ZH, Fang ZP. Char barrier effect of graphene nanoplatelets on the flame retardancy and thermal stability of high-density polyethylene flame-retarded by brominated polystyrene. J Appl Polym Sci 2014;131.
[13] Lautenberger C, Fernandez-Pello C. Generalized pyrolysis model for combustible solids. Fire Saf J 2009;44:819–39.
[14] International Organization for Standardization. Reaction-to-fire tests – heat release, smoke production and mass loss rate – Part 1: heat release rate (cone calorimeter method) ISO 5660-1:2002. 2002.
[15] Bao CL, Guo YQ, Song L, Kan YC, Qian XD, Hu Y. In situ preparation of functionalized graphene oxide/epoxy nanocomposites with effective reinforcements. J Mater Chem 2011;21:13290–8.
[16] Dittrich B, Wartig KA, Hofmann D, Mulhaupt R, Schartel B. Flame retardancy through carbon nanomaterials: carbon black, multiwall nanotubes, expanded graphite, multi-layer graphene and graphene in polypropylene. Polym Degrad Stabil 2013;98:1495–505.
[17] Kumar A, Chouhan DK, Alegaonkar PS, Patro TU. Graphene-like nanocarbon: an effective nanofiller for improving the mechanical and thermal properties of polymer at low weight fractions. Compos Sci Technol 2016;127:79–87.
[18] Osman MA, Mittal V, Morbidelli M, Suter UW. Epoxy-layered silicate nanocomposites and their gas permeation properties. Macromolecules 2004;37:7250–7.
[19] https://www.engineeringtoolbox.com/gases-absolute-dynamic-viscosity-d_1888.html (accessed Nov 15 2017).
[20] Han JH, Cho KW, Lee KH, Kim H. Porous graphite matrix for chemical heat pumps. Carbon 1998;36:1801–10.
[21] Stoliarov SI, Crowley S, Walters RN, Lyon RE. Prediction of the burning rates of charring polymers. Combust Flame 2010;157:2024–34.
[22] Hurley MJ, Gottuk DT, Hall Jr. JR, Harada K, Kuligowski ED, Puchovsky M, Torero JL, Watts Jr. JM, Wieczorek CJ. SFPE handbook of fire protection engineering. Springer; 2015.
[23] Wang LL, Wang YC, Yuan JF, Li GQ. Thermal conductivity of intumescent coating char after accelerated aging. Fire Mater 2013;37:440–56.
[24] Staggs JEJ. Heat and mass transport in developing chars. Polym Degrad Stabil 2003;82:297–307.
[25] Asaro RJ, Lattimer B, Mealy C, Steele G. Thermo-physical performance of a fire protective coating for naval ship structures. Compos Part a-Appl S 2009;40:11–8.
[26] Faghri M, Sundén B. Transport phenomena in fires. Southampton, UK: WIT Press; 2008.
[27] Lautenberger C. A generalized pyrolysis model for combustible solids, mechanical engineering Doctoral dissertation Berkeley: University of California; 2007
[28] Di Blasi C, Branca C. Mathematical model for the nonsteady decomposition of intumescent coatings. AIChE J 2001;47:2359–70.
[29] Lo SK, Tseng CJ, Tsai LD, Lin JN. Fractal permeability models for the microporous layer and gas diffusion layer of PEM fuel cell. J Chin Inst Eng 2011;34:39–47.
[30] Compton OC, Kim S, Pierre C, Torkelson JM, Nguyen ST. Crumpled graphene nanosheets as highly effective barrier property enhancers. Adv Mater 2010;22:4759–63.
[31] Choudalakis G, Gotsis AD. Permeability of polymer/clay nanocomposites: a review. Eur Polym J 2009;45:967–84.
[32] van Rooyen LJ, Karger-Kocsis J, Kock LD. Improving the helium gas barrier properties of epoxy coatings through the incorporation of graphene nanoplatelets and the influence of preparation techniques. J Appl Polym Sci 2015;132.
[33] Fredrickson GH, Bicerano J. Barrier properties of oriented disk composites. J Chem Phys 1999;110:2181–8.
[34] Sun LY, Boo WJ, Clearfield A, Sue HJ, Pham HQ. Barrier properties of model epoxy nanocomposites. J Membr Sci 2008;318:129–36.
[35] Bharadwaj RK. Modeling the barrier properties of polymer-layered silicate nanocomposites. Macromolecules 2001;34:9189–92.
[36] Lusti HR, Gusev AA, Guseva O. The influence of platelet disorientation on the barrier properties of composites: a numerical study. Model Simul Mater Sc 2004;12:1201–7.
[37] Xu B, Zheng Q, Song YH, Shangguan Y. Calculating barrier properties of polymer/clay nanocomposites: effects of clay layers. Polymer 2006;47:2904–10.